Edinburgh, Scotland
EURONOISE 2009
October 26-28

Adventures in active noise control

Colin H. Hansen,
AVC Group, School of Mechanical Engineering
University of Adelaide SA 5005 Australia

ABSTRACT

A brief review of the work in active noise control undertaken by the author and his colleagues at the University of Adelaide during the past 20 years is discussed with emphasis on practical issues associated with the implementation of real working systems. Aspects covered include sensors, speakers, controller hardware, software and physical system configuration Ongoing research at the University of Adelaide is discussed briefly, with a special focus on fixed and moving virtual sensing.

1. INTRODUCTION

Why do we undertake research in acoustics? The world is suffering some immense problems such as a global financial crisis, food shortages, fresh water shortages, environmental pollution, global warming and associated weather extremes, over population, limited traditional energy supplies and erosion of our quality of life due to increased population densities and the associated excessive noise. Solving these problems will require a concerted effort from the best minds we can gather and some may believe that all of us could be of more use to humanity if we re-directed our efforts accordingly. In these hard financial times, it is not difficult to imagine that funding for research in acoustics may become more scarce due to the perceived lack of importance of the discipline in solving these critical problems, However, research in acoustics has a very important role to play in assisting mankind to meet some of the challenges mentioned above and it is essential that this is understood by government and industry so that funding for acoustics research continues to be available from sources other than defence.

Some of the current acoustics research has direct application to the challenges outlined above and much of it has indirect application in that it provides the basic foundation and building blocks that support the more directly relevant applications. Examples of the more directly relevant applications include: thermo-acoustics for refrigeration and air conditioning, using waste heat as the energy source; ultrasound for medical imaging, making diagnosis of medical conditions faster and more accurate; ultrasound for blue green algae control in drinking water storages, eliminating the need to use toxic and environmentally degrading copper sulphate; architectural and virtual acoustics to model and improve the acoustical quality of entertainment venues as well as the acoustical environment in which we live; seismic exploration and earthquake monitoring; and finally (and perhaps most importantly) noise control applications that address the ever growing problem of noise pollution that threatens the quality of life and in many cases the health of such a huge proportion of the world's population and would rate as one of the more serious examples of environmental pollution that we face today.

This paper is focussed on active noise control, which is one sophisticated approach that may be taken to control environmental and occupational noise in situations where it is not possible or practical to implement traditional passive control. Active noise control is a discipline that combines acoustics with signal processing, algorithm design, computation and DSP based electronic hardware. There are many separate aspects that have been the subject

of a large volume of research papers by many researchers. As we all know, active noise control (ANC) is only seriously considered for applications where passive control is impractical or technically infeasible. However, many such situations do exist, but the complexity of implementing practical active noise control systems has so far limited their commercial application. Nevertheless, ANC has an important role to play in reducing environmental noise pollution and the challenge is to translate the excellent research on the topic into practical systems that can be implemented easily by non-experts.

What is needed to generate a significant increase in the use of active control technology is the availability of inexpensive, clever, commercial control systems that include a selection of source and sensor transducers to satisfy most problems as well as software to guide users in the correct choice and location of such transducers. The word "clever" is used above to describe a commercial control system that does not yet exist and needs some explanation. If a controller is to be useful to a wide range of people, the effort involved in setting it up must be very small. This means that the controller must itself be controlled by a high level expert system or neural network that automatically sets input and output gains to maximise system dynamic range, convergence coefficients to optimise convergence speed and stability trade-offs, control filter type and weight numbers to optimise noise reduction, as well as leakage coefficients and system ID algorithms, filter types and configurations to maximise controller performance and stability. In addition, the controller should also be able to perform as an adaptive feedforward or adaptive feedback controller, be extendable to a large number of channels simply by adding together identical modules and provide advice on the suitability of feedforward control compared to feedback control based on the quality of the available reference signal. Finally the controller/user interface during set-up (which should really be a question/answer session) should be Windows based for maximum flexibility. The ability to connect a modem to the controller to allow remote access and interrogation of current performance and the state of transducers and other system components is also an important labour saving device. Also, to make the controller more universally useful, it should be capable of being programmed with new algorithms and filters by anyone with a knowledge of the "C" programming language.

Software must also be developed which is user friendly and allows the user to determine optimum control source and error sensor types, configurations and locations based on measured transfer functions between potential control source and error sensor locations as well as a measure of the primary field strength at these locations.

Designing an active noise control system for use in an industrial environment requires the integration and optimisation of several sub-systems and as such may be regarded as an excellent example of systems engineering. The size of the task is an order of magnitude greater than setting up a laboratory demonstrator, where the operator is present to reset the system should it suddenly become unstable. Some of the additional aspects that need to be taken into account include environmental protection for transducers, minimization of flow noise in reference and error microphones, finding a suitable reference signal that is isolated from the control sources, handling large transient signals from the error microphones, temporary power failures, transducer failures, control system component failures and algorithm instability. With any problem or failure, it is essential that noise levels do not increase over and above what they would have been in the absence of active control. Ways that have been used to overcome these problems are discussed in following sections.

The differences between feedforward and feedback ANC systems have been discussed elsewhere[1,2]. Here only adaptive feedforward control is considered as this is the system that is most likely to produce acceptable results in an industrial environment.

The basic components of an adaptive feedforward active noise control system are shown in Figure 1. A sensor is used to measure an environmental signal that is related in frequency and time to the noise that is to be attenuated. The electrical signal produced by this sensor

is referred to as the reference signal. For practical active noise control systems, it is important that the control source signal does not contribute significantly to the reference signal. This is why tachometer signals related to the shaft speed of rotating machinery generating the unwanted noise are often used when tonal noise is to be reduced. If sound radiation from a vibrating structure is to be reduced using acoustic sources, then an accelerometer on the structure may provide a suitable reference signal as shown in Figure 1. There are ANC algorithms and control filter arrangements available that can be used to cancel the control source signal contribution to the reference signal[3], but these algorithms are not as inherently stable as those suitable for systems with no feedback from the control source to the reference signal.

The ANC algorithm and control filter are responsible for generating the noise cancelling signal. The error sensor senses the residual sound field made up of a combination of the original noise and the noise produced by the control source. This error signal is then used as

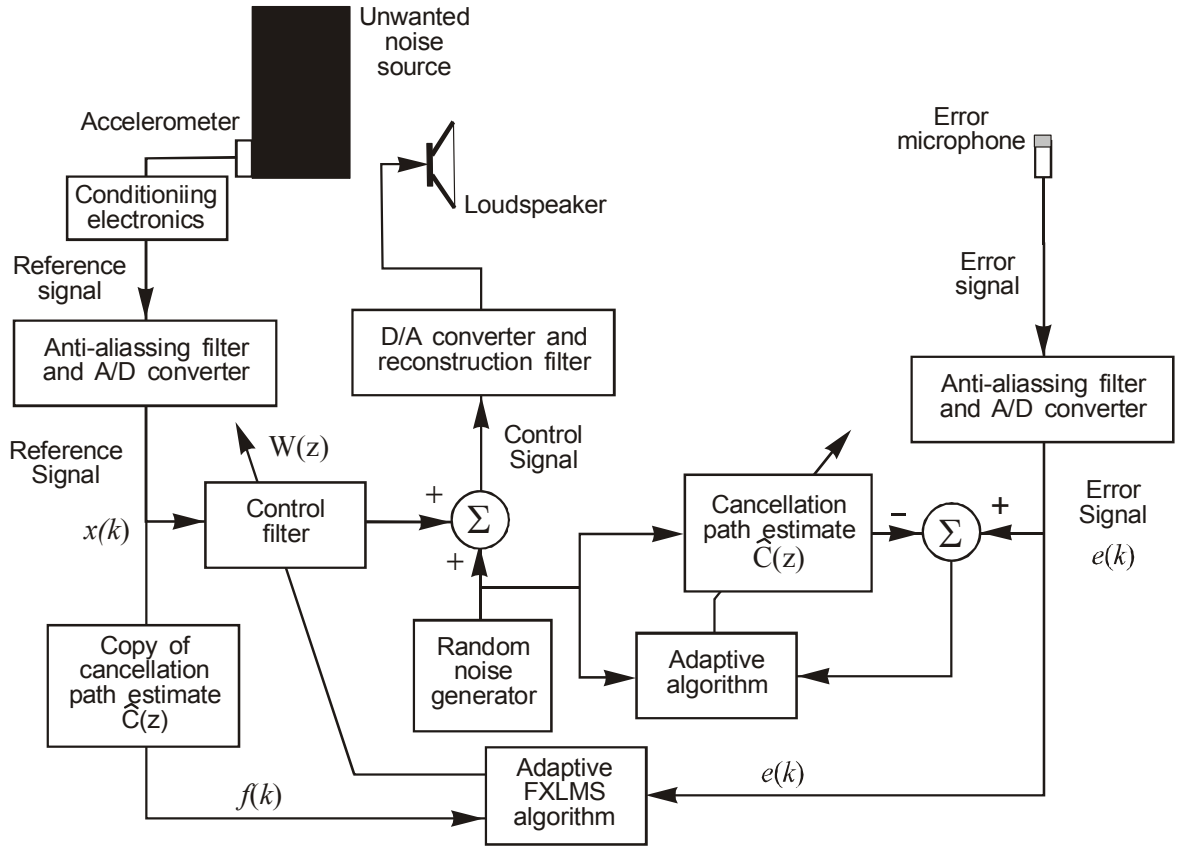

Figure 1: Typical control system layout with on-line cancellation path identification.

an input to the control algorithm, which in turn produces the updated filter coefficients for the control filter. The signal produced by the control filter is modified as it travels from the control source input to the error sensor output. The extent of this modification has to be measured and the reference signal has to be modified in the same way before it is passed into the control filter to be combined with the error signal to produce the control signal. This is done by passing the reference signal through a filter known as the cancellation path filter and the coefficients of this filter are determined by measuring the cancellation path transfer function or impulse response. The impulse response can be measured off-line or on-line. The "off-line" measurement is done with the ANC system turned off and can be done by injecting random noise into the control loudspeaker. This approach is adequate if the environmental conditions

such as temperature as well as the control source and error sensor characteristics do not vary much over time. Alternatively, the cancellation path impulse response can be measured by injecting a very low level random noise signal into the control source and using a long time average to determine the impulse response while the ANC system is running. This allows the estimation of the cancellation path impulse response to be continuously updated and is referred to as "on-line cancellation path ID". As will be shown, this cancellation path is represented by a finite impulse response filter with coefficients that make it behave in the same way as the cancellation path in terms of its effect on an input signal. The coefficients of this cancellation path filter are an important part of most ANC algorithms and best results are obtained if these can be continuously updated.

The signal processing time of the controller must be less than the time for the acoustic signal to propagate from the reference sensor to the control source for broadband noise control, but for tonal noise control, there is no maximum permitted processing time as the signal is repetitive.

It is useful to explore the physical limitations associated with active noise control systems. There are essentially three different physical mechanisms that provide the measured noise reduction. In some situations, all of the three mechanisms can work either alone or together. In other situations, only one mechanism is possible and the system has to be set up to take maximum advantage of it. The three mechanisms are cancellation, reflection and impedance unloading.

With the cancellation mechanism, the acoustic field is cancelled in some locations by the control source but conservation of energy dictates that there must be other parts of the sound field where the sound pressure increases to compensate.

The reflection mechanism is really only relevant in waveguide systems such as ducts and mufflers. In this situation, the control source can create an impedance mismatch much like a reactive muffler does, and reflect the acoustic energy back upstream towards the source.

The final mechanism, impedance unloading, is the only mechanism (except for the application of control of noise radiated from the exit of exhaust ducts) by which global noise reduction can be achieved with an active noise control system involving only sound sources as control sources. In this case the control source is placed in a location where it can reduce the radiation impedance that is "seen" by the primary source and thus reduce the total sound power radiated by the primary source / control source combination. When the primary source is out of doors, the only way that a control source can significantly affect its radiation impedance is if it is placed close to the primary source. If the primary source is large, then it will require multiple control sources to be placed around the primary source with no more than half a wavelength between the control sources. If the source is in a waveguide, then it is possible for a control source placed in the waveguide to affect the radiation impedance of a source at some other location in the waveguide. If the primary source is in a fairly live room, then it will be exciting resonant modes in the room and a control source will be effective in affecting the primary source radiation impedance if it is placed at a location in the room where it can drive the same modes (or a subset of them) that are driven by the primary source.

Of course, if the unwanted sound is a result of vibration of a structure or excitation of a structure by a machine, active systems can be used to reduce the structural vibration or the transmission of vibratory energy from the energy source to the structure and this can also result in global reduction of the resulting sound field.

2. ANC SYSTEM IMPLEMENTATION IN AN INDUSTRIAL ENVIRONMENT

In this section we consider each of the components making up an active noise control system and in particular will focus on what is needed for the various components to enable an active noise control system to function in an industrial environment. The discussion on reference sensing will be followed by a discussion of control algorithms, controller hardware, control

system configuration and sound sources and sensors. Finally some examples of prototype industrial systems will be discussed.

A. Reference Signal Derivation

There are many ways that can be used to generate a reference signal. For the control of tonal noise, these include wrapping a coil around a power cable (electrical transformer noise control) and use of a magnetic or optical tachometer when the noise source is related to the rotational speed of rotating machinery. For control of random noise, if the noise source is a vibration structure, an accelerometer on the structure may be useful. Alternatively a microphone may have to be used and in this case it is important that the feedback from the control source to the reference sensor is minimised. In most cases where a microphone is used as the reference sensor, it will be necessary to use a control filter arrangement and associated algorithm that can compensate for this feedback and cancel it from the reference signal.

With all reference signals, it is important that care is taken to avoid the signal being contaminated by electrical noise associated with nearby equipment - especially when long leads are used to connect the reference signal to the controller. It is important that tacho signals are passed through a low pass filter to eliminate higher order harmonics, unless these harmonics actually exist in the unwanted noise. A potentially useful method for transmitting the reference signal (or error signals) from the sensor location to the control system location is to use radio transmitters. This eliminates the need for hard wired connections and all of the associated problems that occur in an industrial environment.

B. Control Filters and Basic Algorithms

For a time domain system, the electronic controller for the single channel system shown in Figure 1 consists of an analog to digital converter for the reference signal and one for the error signal. The reference signal is passed through a digital filter to produce the control signal for the loudspeaker which is passed through a digital to analog converter and smoothing filter prior to being fed into the loudspeaker amplifier. The digital filter weights (w_0 to w_{L-1}) shown in Figure 2[1] are adjusted by an algorithm that uses the reference and error signals as inputs. The algorithm also needs to take into account the impulse response of the path between the control source output from the controller and the error microphone input to the controller. Estimation of the characteristics of this path is known as "cancellation path modelling" and finding more effective ways of doing this is one area of continuing research. The simplest type of digital filter used in ANC systems is the finite impulse response (FIR) filter illustrated in Figure 2. In the figure, z^{-1} represents a delay of one (input) sample, $x(k)$ is the input signal at time sample, k and w_i represents filter weight i. The structure in Figure 2 is sometimes referred to as a transversal filter, or a tapped delay line. The number of "stages" in the filter (the number of present and past input samples used in the output derivation) is usually referred to as the number of filter "taps".

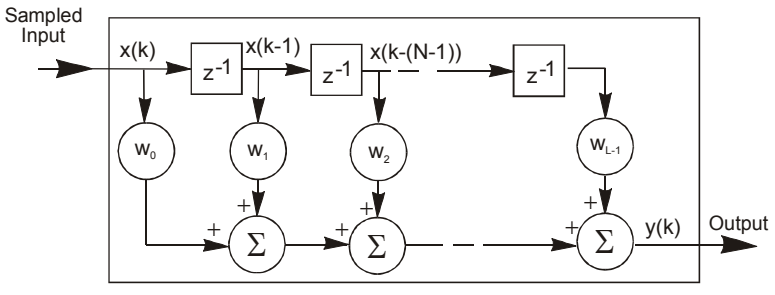

Figure 2: FIR filter architecture.

The filter weights are updated at each time sample using the following equation[1]:

$$\boldsymbol{w}(k+1) = \boldsymbol{w}(k)[1 - \mu\alpha] - 2\mu e(k)[\boldsymbol{c}(k) * \boldsymbol{x}(k)] \quad (1)$$

where $\boldsymbol{x}(k) = \{x(k)\ x(k\text{-}1)\ \cdots\ x(k\text{-}L\text{+}1)\}$, $\boldsymbol{w}(k)$ is the vector of length, N, of filter weights at time, k, $e(k)$ is the error signal at time, k, $\boldsymbol{c}(k)$ represents the coefficients or weights (total number, L) of the FIR filter used to model the cancellation path[1], α is a leakage coefficient to prevent weight build up as a result of quantisation errors and μ is the convergence coefficient. The asterisk represents the convolution operation. This filter weight update equation is referred to as the filtered-x leaky LMS algorithm. If the α parameter were set equal to zero, it would be called the filtered-x LMS algorithm. In many cases it is desirable to normalise μ with the reference signal as follows:

$$\mu = \frac{\beta}{\boldsymbol{x}^{\mathrm{T}}(k)\,\boldsymbol{x}(k)} \tag{2}$$

where β is a constant between 0 and 2. When this is implemented, the algorithm is called the normalised filtered-x LMS algorithm.

Another filter type that is commonly used where there is a possibility that the reference signal may be contaminated by the control source sound is an IIR filter, which has a structure that attempts to compensate for the feedback from the control source to the reference sensor[3,4,5].

C. Advanced Algorithms

It is clear that cost effective operation of practical systems requires algorithms that are more capable than the basic algorithms discussed in the previous section. To increase the upper limiting frequency and bandwidth of a feedforward control system, a higher system sampling rate often has to be used, and this brings a significant computational load, which precludes their use for many low-cost applications.

For example, consider a single channel active noise control system in a duct, where the impulse response from the control source to the error sensor is about 0.25s due to the reflections from the ends of the duct. If the noise to be controlled is below 500Hz, the sampling frequency can be as low as 1000Hz, and the length of the FIR filter for modelling the cancellation path should be about 250 taps. However, if the noise components to be controlled are up to 5000Hz, then the sampling frequency needs to be 10000Hz, and the length of the cancellation path FIR filter should be about 2500 taps. For a typical DSP processor, usually 1 instruction cycle is needed for one tap FIR filtering operation and 2 instruction cycles are needed for one tap LMS update operation; thus at least 7500 instruction cycles are needed for the control filter update of the single channel ANC system which has the FXLMS algorithm implemented. If the system needs to be updated every sample, this requires the processing capability of the DSP processor be greater than 75MFLOPS, ten times higher than that of the system with 1000Hz sampling frequency.

A number of algorithms have been proposed to reduce the computation load of the FXLMS algorithm. For example, the block FXLMS algorithm uses the sum of the mean-square errors over a period of samples as its cost function, resulting in less frequent update on block by block basis; the periodic FXLMS algorithm reduces the computational load by updating the filter coefficients every N samples with the Nth samples, and the periodic block algorithm is a combination of the previous two, which updates the filter coefficients every N samples with a small block of data where the block size is much smaller than that of the block FXLMS algorithm, but larger than the number of samples in a period of the disturbance. The frequency domain algorithm can also be used, which involves implementation of the control filtering in the time domain and updating of the control filter coefficients in the frequency domain.

With the above algorithms, the computation load can be substantially reduced, yet there are still some problems associated with each of them. For example, the periodic FXLMS algorithm may suffer from a long convergence time, and the implementation of the frequency

domain algorithm may need large on-chip memory. There is another kind of time and frequency domain algorithm called the sub-band FXLMS algorithm. With this approach, the input signals from the reference and error sensors are sampled at a high frequency and filtered into many sub-bands. Each sub-band signal is then phase-shifted and down-sampled at a lower sampling rate and then processed to frequency shift it to a base band, which spans a frequency range from 0 Hz to an upper frequency that is dependent on the original sampling rate and the number of sub-bands used to divide up the frequency range of interest. For each sub-band, an adaptive control filter is used to provide the sub-band control signal, and the signals from each sub-band are combined and up-sampled to synthesize the full-band control signal. If each sub-band is characterised by different energy levels, then the control system performance can be optimised for maximum convergence speed in each sub-band by using a filtered-X normalised LMS (FXNLMS) algorithm where the convergence coefficient is normalised by the band signal power.

Applying sub-band signal processing techniques in active noise control has several advantages. For example, the high sample rate sometimes can eliminate the need for sharp anti-aliasing filters and reduces the inherent one sample delay of the digital system. Each sub-band can have its own convergence coefficients and the signal dynamic range is greatly reduced in each sub-band, so the whole control system is likely to converge faster and track more quickly. However, the most important advantage is that the computation complexity for the control filter update can be greatly reduced by approximately the number of the sub-bands due to the reduced number of filter taps and weight update rate in each sub-band. For narrow band noise, both the computation complexity and the memory requirement can be further reduced.

The delayless sub-band adaptive architecture for the FXLMS algorithm was proposed by Morgan and Thi[6,7] and extended to multi-channel systems by Qiu et al[8]. Figure 3 shows the structure of the single channel delayless sub-band ANC system with the physical cancellation path transfer function $C(z)$, which is modelled by injecting uncorrelated random noise $r(n)$ into the system. $x(n)$ is the reference signal from the noise source and $P(z)$ is the primary path transfer function between the primary noise $p(n)$ and $x(n)$. The output of the controller $W(z)$ is $y(n)$, and the error signal $e(n)$.

The system consists of 5 parts: sub-band signal generation; sub-band cancellation path modelling; sub-band adaptive weight update; sub-band/full-band weight transformation; and full-band control signal generation (control filtering). All of these are described below. The main difference between the sub-band algorithm and the common full-band FXLMS algorithm, is that, except for the control signal generation, which is carried out in full-band to avoid delay, all parts of the control system operate in each sub-band at a decimated sample rate. This reduces the computation load and allows independent and different convergence coefficients, thus allowing the controller to operate over a wider bandwidth. Note that the same sample rate is used on each sub-band, as frequency shifting is carried out on each band before down sampling so that all bands are processed in the base band. In all of the following, it is possible to replace the FXLMS algorithm with the normalised algorithm. Thus, if each sub-band is characterised by different energy levels, then the control system performance can be optimised for maximum convergence speed in each sub-band by using a filtered-x normalised LMS (FXNLMS) algorithm where the convergence coefficient is normalised by the band signal power.

As an example consider a 16kHz sampling frequency and a frequency range of interest of 0 to 4000Hz. If the sample rate is down-sampled to 250Hz for the sub-bands, then this implies that there will be 64 sub bands (16000/250). The maximum frequency for each sub-band is half the sampling frequency; that is, 125Hz. As the upper frequency of interest is 4000Hz, only the first 32 sub-bands need to be processed (4000/125 = 32), which, for a 4000Hz band-width divided into 64 sub-bands, is 0-125Hz. Note that it is possible to over

sample and still have the same number of sub-bands so that many more samples are taken for each cycle. In the current example, if we wanted to sample at 10 times the upper frequency of the sub-band, we still could do that and have the same number of sub-bands. This would give better results at the lower end of each sub-band.

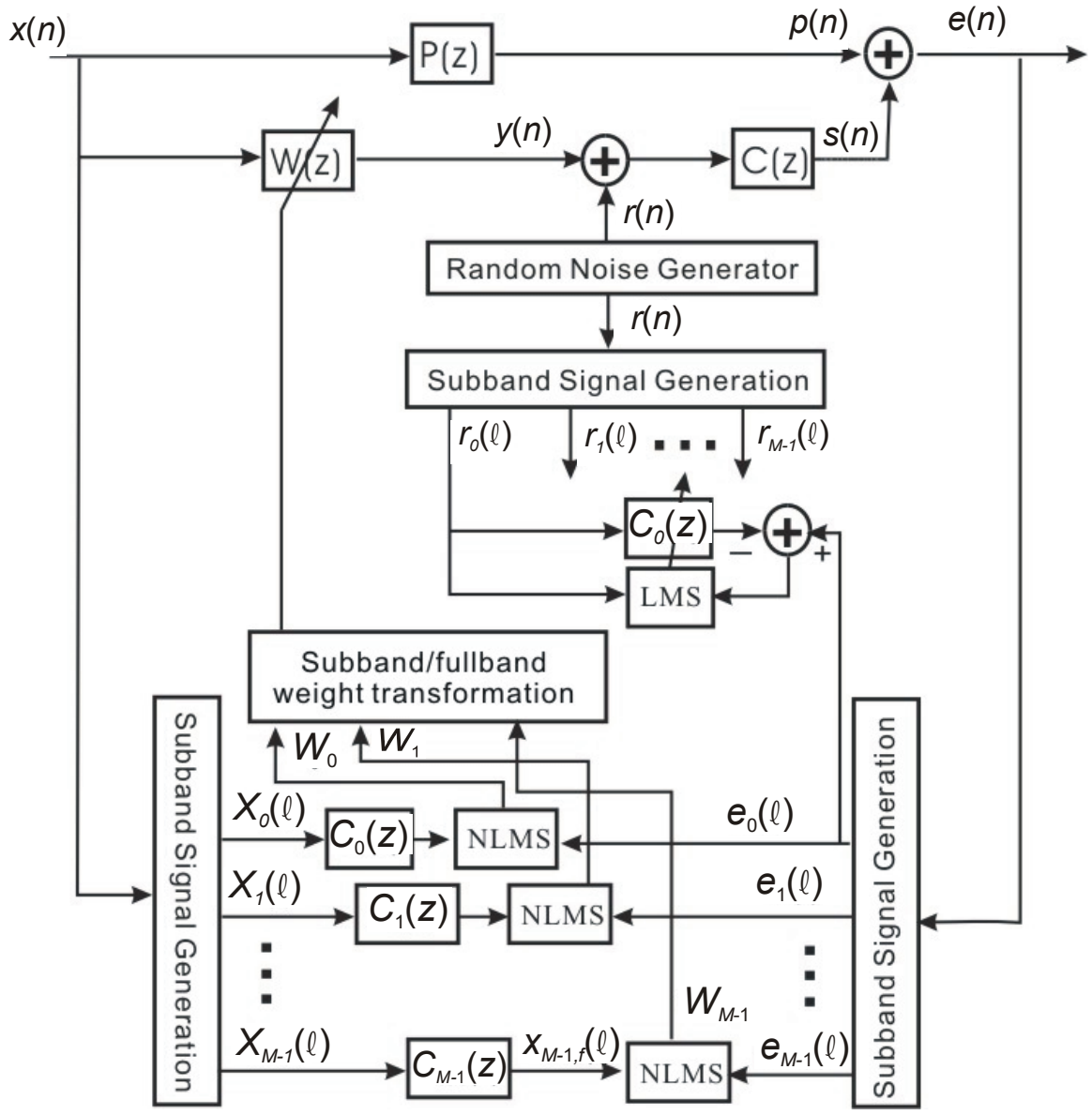

Figure 3: Delayless sub-band ANC system using the FXLMS algorithm.

The procedure for generating the sub-band signals will now be discussed. The *m*th sub-band signal $x_m(\ell)$ is calculated by bandpass filtering, frequency shifting, and down sampling the full-band signal $x(n)$,

$$x_m(\ell) = \sum_{k=0}^{K_L-1} a_k e^{-j2\pi\frac{mk}{M}} x(D\ell - k) = \sum_{k=0}^{M-1} a_k e^{-j2\pi\frac{mk}{M}} \sum_{n=0}^{K_L/M-1} a_{k+nM}\, x(D\ell - k - nM) \qquad (3)$$

where ℓ is the sub-band index, D is the down sampling frequency, a_k are the coefficients of

a K_L point low pass prototype FIR filter and K_L is usually larger than the number of sub-bands M to avoid aliasing. The calculation complexity for all sub-band signal generation can be reduced by using the polyphase FFT method:

$$[x_0(\ell) \quad x_1(\ell) \quad \cdots \quad x_{M-1}(\ell)]^{\mathrm{T}} = FFT\{\mathbf{F}\,\boldsymbol{x}(\ell)\} \tag{4}$$

where the K_L point column vector $\boldsymbol{x}(\ell) = [x(D\ell) \quad x(D\ell - 1) \quad \cdots \quad x_{K-1}(D\ell - K_L + 1)]^{\mathrm{T}}$, the prototype filter matrix $\mathbf{F}$ is of size $M \times K_L$, and an example with $M = 4$ and $K_L = 8$ is shown below.

$$\mathbf{F} = \begin{bmatrix} a_0 & 0 & 0 & 0 & a_4 & 0 & 0 & 0 \\ 0 & a_1 & 0 & 0 & 0 & a_5 & 0 & 0 \\ 0 & 0 & a_2 & 0 & 0 & 0 & a_6 & 0 \\ 0 & 0 & 0 & a_3 & 0 & 0 & 0 & a_7 \end{bmatrix} \tag{5}$$

The D new input samples are shifted into $\boldsymbol{x}(\ell)$ and multiplied with the prototype filter matrix $\mathbf{F}$. The M sub-band signals are obtained by applying a FFT to the obtained M-point product. In the algorithm shown in Figure 3, the reference signal, the error signal and the modelling signal are all decomposed into sub-band signals using this method. The generated sub-band signals are complex values, so complex valued adaptive filters are needed. However, as the full-band signal and the prototype filter matrix are real values, it is only necessary to do the calculation for the first M/2+1 sub-bands.

Figure 3 also illustrates the method used to obtain the sub-band cancellation path transfer functions where the modelling signal $r(n)$ (random noise) is decomposed into M sub-band modelling signals, which are used with the M sub-band error to directly obtain the sub-band cancellation path transfer functions. The update equation for the sub-band FXLMS algorithm in each sub-band is almost the same as that of full-band FXLMS algorithm, except that complex valued filtering and the LMS algorithm have to be used.

The purpose of the sub-band/full-band filter weight transform is to transform a set of M sub-band filter weights $\mathbf{W}_m$ of length N_s, into a corresponding full-band filter $\mathbf{W}$ of length N. Several methods have been developed, such as the DFT stacking method, the DFT-2 stacking method, the DFT-FIR weight transform and the linear weight transform. For example, by using the DFT-FIR weight transform, the full-band filter weights are obtained by using the sub-band filter weights as input sub-band signals to the synthesis filters. The full-band signal (weights) can be obtained by summation of all the sub-band signals after up sampling, bandpass filtering and frequency shifting.

It should be noted that the maximum computation complexity reduction of the single channel delayless sub-band ANC system with the FXLMS algorithm is only about 33% of that of the full-band FXLMS algorithm due to the delayless requirement. However, the computation complexity reduction provided by the multi-channel delayless sub-band ANC system with the MFXLMS (multi-channel FXLMS) algorithm can be much more. The multi-channel sub-band ANC system consists of the same 5 parts as the single channel case: cancellation path modelling; adaptive weight updating; and sub-band/full-band weight transformation. These steps are all carried out in each sub-band at the reduced sampling frequency to reduce the computation load, and only multi-channel control signals are generated by full-band FIR filters to avoid delay. Figure 4 shows the ratio of the computation complexity of the sub-band MFXLMS to the full-band MFXLMS when the sub-band number is 32, 64, 128, 256 and 512 as a function of the number of the control channels. In this case, the length of the control filter and cancellation path filter are 4096, with two times over sampling in the sub-bands (D=M/2). The length of the prototype filter is 4 times that of the sub-band number. It can be seen that with the increase of sub-band number, the computation load of the sub-band MFXLMS

algorithm with a large number of channels can be reduced to about 8/M of that of the full-band. It can also be seen that when *M* is larger than a particular value, further increasing *M* cannot further reduce the computation load of the sub-band algorithm significantly, as the main contributor to the computation load becomes the control signal generation part at full-band.

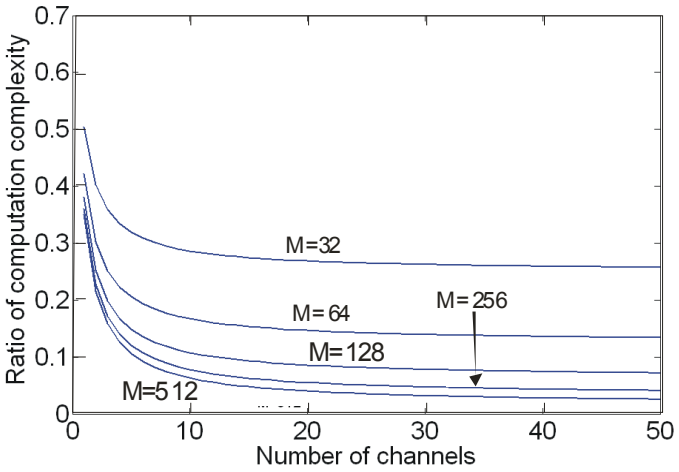

Figure 4: The ratio of the computation complexity of the sub-band to the full-band MFXLMS as a function of the number of the control channels for different numbers of sub-bands, *M*.

One alternative solution to the sub-band approach discussed above is to use frequency domain, multi-delay adaptive filters. The multi-delay adaptive filter (MDF) is a flexible structure, which partitions a long filter into many shorter sub-filters so that a much smaller size of FFT can be used to reduce the delay and memory requirements while maintaining the low computational complexity and faster convergence properties of the frequency domain algorithm. This approach, including taking into account the cancellation path transfer function has been discussed in detail by Qiu and Hansen[9].

Table 1: The average number of real multiplications required per input sample to implement various FXLMS algorithms.

	Control filter filtering	filtered-x signal generation	Control filter update	Transformation	Total
TD FXLMS	L	L	L	0	$3L$
FD FXLMS	8	8	8	$14\log_2 2L$	$24+14\log_2 2L$
DFD FXLMS	L	8	8	$14\log_2 2L$	$16+14\log_2 2L+L$
Delayless subband	L	$2LK/D^2$	$2LK/D^2$	$3(K_L+K\log_2 K)/D$	$3(K_L+K\log_2 K)/D$ $+4LK/D^2+L$
MDF FXLMS	$8K$	$8K$	$8K$	$14\log_2 2N$	$24K+14\log_2 2N$
Delayless MDF	$N+8(K-1)$	$8K$	$8K$	$16\log_2 2N$	$24K+16\log_2 2N+$ $N-8$

In the table, L is the number of samples in the FFT block prior to partitioning into multi-delay adaptive sub-filters, K is the number of sub-filters after partitioning, N is the number of samples in the partitioned block ($N << L$), K_L is the number of taps in the sub-band filters and D is the down sampling frequency. The terms TD, FD and DFD FXLMS in the table represent, respectively, the time domain, frequency domain and traditional delayless constrained frequency domain FXLMS algorithm[10]. For the table, it is assumed that $2N\log_2 2N$ real multiplications are required for a $2N$ point FFT or IFFT, and $8N$ real multiplications are required for $2N$ complex multiplications in the frequency domain FIR filtering or LMS update.

D. Controller Hardware

Continuing advances in computer processor power and reductions in costs of this power and advances in actuator and sensor technology are also helping to make active control technology more practical and affordable.

One of the most difficult issues facing researchers and consultants in the active control field is the large development time needed to keep up with advances in processing speed and memory capability of the electronic hardware used to implement the control systems. Modern DSP chips have such a high pin density that printed circuit board manufacture requires special expensive tooling which is only economical if boards are manufactured in large quantities.

There are currently four possible paths that may be followed in the hardware development for a new active noise controller. These are: (1) use currently available commercial general purpose DSP systems that can be programmed for ANC in a high level language such as C; (2) use a standard input/output board embedded in a PC and an operating system dedicated to real time processing; (3) use a general-purpose DSP board in a custom enclosure with power supply and custom I/O boards (4) develop a multi-processor DSP board from scratch with sufficient power and memory to meet the most demanding ANC application. Include it in a modular system that allows the use of multiple DSP boards and multiple IO modules, which can be tailored to the number of channels needed and the processing power and memory required.

Although the fourth option offers more flexibility in terms of producing a system optimised for active noise and vibration control, it needs considerably more effort and financial resources. Generally, options (1) and (2) above are usually suitable only for laboratory demonstrations. Option (3) could potentially be used to develop commercial systems, but the available general purpose DSP boards are difficult to use and interfacing them with other hardware usually results in numerous problems. In addition they are usually based on out of date DSP chips. Option (4) above is the best approach as the most up to date DSP chips can be used and the hardware can be optimised for ANC applications, provided that there are sufficient time and financial resources available. As option (3) is the least useful, it will not be discussed further here. The most well known system that may be classified as option (1) is d-Space, provided by the MathWorks company. This system is used by many researchers and will not be discussed further here.

Option (2) uses a standard Input/output card in a PC and an Operational System (OS) and Freeware (QNX or Linux) dedicated to real-time processing. It can be installed on any general-purpose computer. The advantage of this approach is that it allows the design of embedded systems for direct application of the type FPGA (Field Programmable Gate Array), without requiring the designer to have knowledge of machine language (VHDL). This technology is currently rarely used because it is still new, but the interest from industry has been growing considerably in the past several years as its viability increases with dropping costs. The most well-known software engines are XPCTarget and RT-LAB provided by MathWorks and Opal-rt respectively. The intention of these software packages is to overcome the restrictions of real-time operation using other software that is already well developed from the theoretical point of view in the areas of mathematical calculations, signal processing and automation. One of the original aspects of RT-LAB is the use of a cross-platform, open-source scripting language called Python, whose use is growing in popularity, particularly for technical applications. Its syntax is very close to m-script, which has become very popular among Matlab users. It is object-oriented and allows users to automate applications on any platform. The RT-LAB API allows users to configure models and automate test runs using the Python language. Also, because Python is multi-threaded, it is possible to interface to multiple concurrent models, running on several target processors. This means that it is possible to program several different tests, and even have data flowing from one test platform to another

from a single operator station. In other words, this functionality allows the generation of a statistical representation of experiment or process behaviour, which is a valuable laboratory tool.

An example of a system that satisfies Option (4) above is illustrated in Figure 5, which shows the architecture of the third generation controller, EZ-ANC III, which is being developed in the University of Adelaide. Each I/O module contains simple signal conditioning hardware such as a two order low pass filter, a short delay A/D and D/A converter sampling at a high frequency and a low cost DSP, which provides ample processing power for the I/O management tasks and multi-rate signal processing as well as transducer failure and signal overload management. The adaptive signal processing and system modelling are carried out in the central processor module, which contains an array or a cluster of DSPs with a huge amount of shared global memory and an interface for a PC.

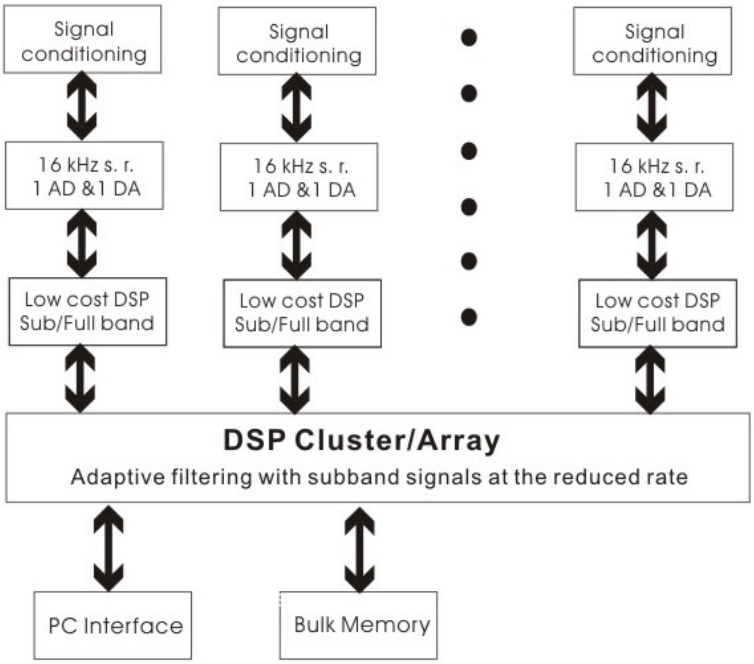

Figure 5: The architecture of the EZ-ANC III.

E. Control System Configuration

The arrangement of the sensors and actuators in an active noise control system is critical. The arrangement of control sources will dictate the maximum global noise control achievable whereas the arrangement of the error sensors needs to be such that the quantity to be minimised is accurately sensed. For, example if sound power radiated from a structure is to be minimised, then sufficient and appropriately arranged acoustic pressure sensors are needed to obtain a good estimate of the radiated sound power. Methods for optimising control sources and error sensors have been discussed elsewhere[1,11,12].

In many industrial environments, it is necessary to locate the controller hardware at some distance from reference sensors, error sensors and control sources. This causes expense and inconvenience in terms of the long lengths of wiring needed to connect everything together. The temptation to route signal and power cables in the same conduits can also be problematical, with the signals becoming contaminated with electrical noise. Although to the author's knowledge, wireless connection of all components has not yet been implemented, it is certainly an option that should be considered as it would eliminate many of the problems associated with wired connections.

F. Error Sensors

The most common error sensors used in active control applications are low cost electret microphones. These may be purchased with power supply for tens of dollars or without cable or power supply for $1. Thus multiple error microphones (for which the outputs are summed) may be used economically to improve system reliability. The author has used these

microphones in very dirty environments using a complex holder that allowed for air purging and also protected the microphone from contamination[13]. The additional noise at the microphone location resulting from the air purge is dependent on the speed of the air flow over the microphone. For the case considered here it was about 85-90dB which was sufficiently below the duct noise that it was not a problem as duct noise levels varied from 112dB to 138dB. In later work, it was found that a simpler holder was adequate for all but the slimiest of environments and this is illustrated in Figure 6. This holder has the added advantage of allowing attenuating inserts to be applied for cases where the duct noise levels exceed the upper range capability of the microphone (often the case when low-cost electrets are used). Electret microphones seem to function adequately for ANC purposes even when covered in dirt.

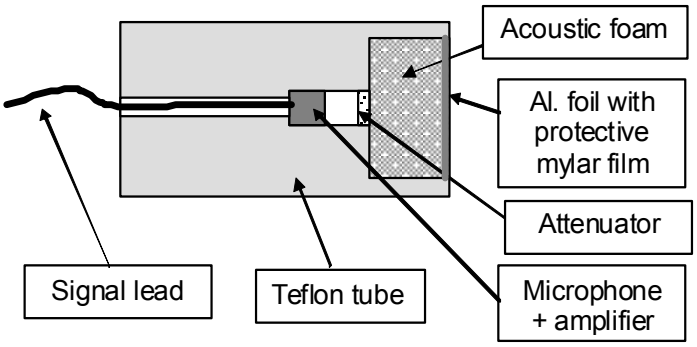

Figure 6: Microphone holder for contaminated environments.

Better results are invariably obtained by ANC systems if all microphone signals are band pass filtered (with either an analog or digital filter) so that they only produce signals to the controller in the frequency range for which ANC is required.

In many cases aerodynamic pressure fluctuations caused by fluid flow and travelling with the speed of the flow contaminate the microphone signals and reduce the achievable noise reduction. This problem can be ameliorated by either using turbulence filters[1] on microphones mounted inside the duct if the flow is uncontaminated or alternatively, the microphone may be located in a small side branch such that the aluminium foil is either flush with the duct or slightly recessed. Note that if a turbulence filter[1] is used, it has the added advantage of making the microphone directional, which is particularly useful in reducing acoustic feedback to the reference microphone from the control sources.

G. Virtual Sensing

This sensing method involves estimating the sound field at a location remote from the physical sensors and using an active control system to minimise the sound field at the remote location. There have been a number of excellent papers published on this topic[13-16] and more recently, the technique has been extended to using fixed microphones to generate a moving virtual microphone[17-20]. Why is a virtual microphone of interest? The reason is that active noise control systems working on the cancellation mechanism can produce a large reduction in sound level at error microphone locations but as one moves away from the error microphone, the noise reduction becomes much less very quickly. In an industrial environment, the desired noise reduction location is often at the ear of a person and it is inconvenient to locate a physical microphone right at their ear. With a fixed virtual microphone, it is possible to obtain maximum noise reduction at the subject's ear using remote physical microphones. However, if the subject moves their head, they will experience large and rapid changes in sound level as they move in and out of the area where the cancellation effect is a maximum. Thus it is necessary for the virtual microphone to be capable of moving with the subject's ear. The location of the ear in 3-D space can be determined using ultrasound[18], much like some cameras do when focussing automatically.

The moving virtual location at time step, k, is defined as a vector $\boldsymbol{r}_v(k)$ of 3 spatial coordinates and it is associated with a virtual signal, $e_v(k)$, estimated using the signals from

a number, M_v, of spatially fixed virtual microphones and the remote microphone technique[14]. The spatially fixed virtual microphone positions may be represented in vector form as:

$$\boldsymbol{r_v} = \{\boldsymbol{r_{v1}} \quad \boldsymbol{r_{v2}} \ \ldots \ \boldsymbol{r_{vM_v}}\} \tag{6}$$

Following the procedure for the remote microphone technique, the impulse response associated with the transfer function between the control source signal, $u(k)$, and the physical microphone output is modelled using an FIR filter, with L fixed filter weights represented as $\boldsymbol{c_{c\,m}} = \{c_{c\,m\,1}\ c_{c\,m\,2}\ \cdots\ c_{c\,m\,L}\}$. The impulse responses associated with the transfer functions between the physical microphone location and each virtual microphone location is modelled using an FIR filter, with J fixed filter weights represented as ($[\boldsymbol{c_{vai}} = \{c_{vai1}\ c_{vai2}\ \cdots\ c_{vaiJ}\}]$, i=1, M) and M is the number of virtual locations. The estimate of the primary disturbance, $p_{pa}(k)$, at time sample, k, at the physical microphone is:

$$p_{pa}(k) = p_a(k) - p_{ca}(k) = p_a(k) - \boldsymbol{c_{cm}} * \boldsymbol{u}(k) \tag{7}$$

where $p_a(k)$ is the total sound pressure at the physical microphone at time k, $p_{ca}(k)$ is the contribution due to the control source and $\boldsymbol{u}(k) = \{u(k)\ u(k\text{-}1)\ \cdots\cdots\ u(k\text{-}L\text{+}1)\}$ is the control source signal.

The sound pressure, $p_{pvi}(k)$ at time k, at a particular virtual location, i due to the primary source is:

$$p_{pvi}(k) = \boldsymbol{c_{vai}} * \boldsymbol{p_{pa}}(k) \tag{8}$$

where $\boldsymbol{p_{pa}}(\mathrm{k}) = \{p_{pa}(k)\ p_{pa}(k\text{-}1)\ \cdots\ p_{pa}(k\text{-}J\text{+}1)\}$. The impulse response associated with the transfer functions between the control source and each virtual microphone location is: $\boldsymbol{c_{vci}} = \{c_{vci1}\ c_{vci2}\ \cdots\ c_{vciL}\}$.Thus the total sound pressure at the virtual location, i, is:

$$p_{vi}(k) = p_{pvi}(k) + p_{svi}(k) = \boldsymbol{c_{vai}} * \boldsymbol{p_{pa}}(k) + \boldsymbol{c_{vci}} * \boldsymbol{u}(k) \tag{9}$$

The sound pressure at all virtual locations is calculated in the same way and then the instantaneous sound pressure (at time step, k) at the moving virtual location is determined by interpolation of the sound pressure at the fixed virtual locations. Of course better results can be obtained by using more than one fixed microphone and this is discussed in detail by Moreau[20]. Another possible way of improving results would be to use energy density sensing and pairs of microphones rather than individual microphones.

The method outlined above was used to force the moving virtual sensing location to track the ear in a rotating head form in a 3-D, modally dense, enclosure as illustrated in Figures 7 and 8.

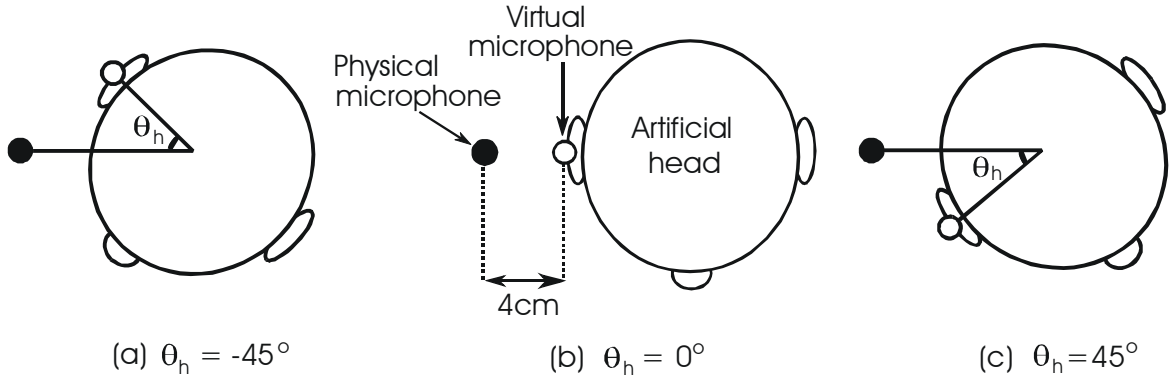

Figure 7: Relationship between the headform and the physical and virtual microphones.

Results obtained are shown in figure 9, where it can be seen that the moving virtual microphone performs much better than a stationary physical microphone and a fixed virtual

microphone in terms of maintaining a relatively steady sound level at the ear and a significant reduction at the same time.

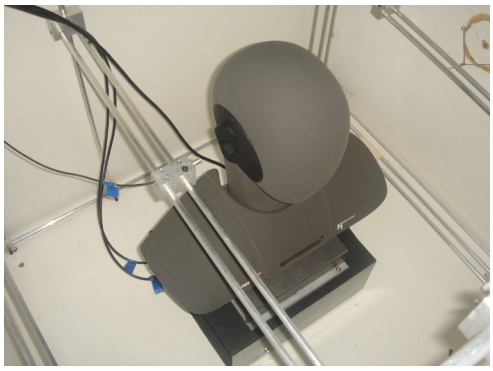

Figure 8: Rotating headform in modally dense enclosure.

H. Sound Sources

In recent times, the availability of new materials has opened up the scope for novel speaker systems suited specifically to active control applications. Loudspeaker cones made from polypropylene, carbon fibre and aluminium are available for hostile environments and low frequency applications. Lower cost alternatives have involved the use of paper cone loudspeakers sprayed first with engine gasket

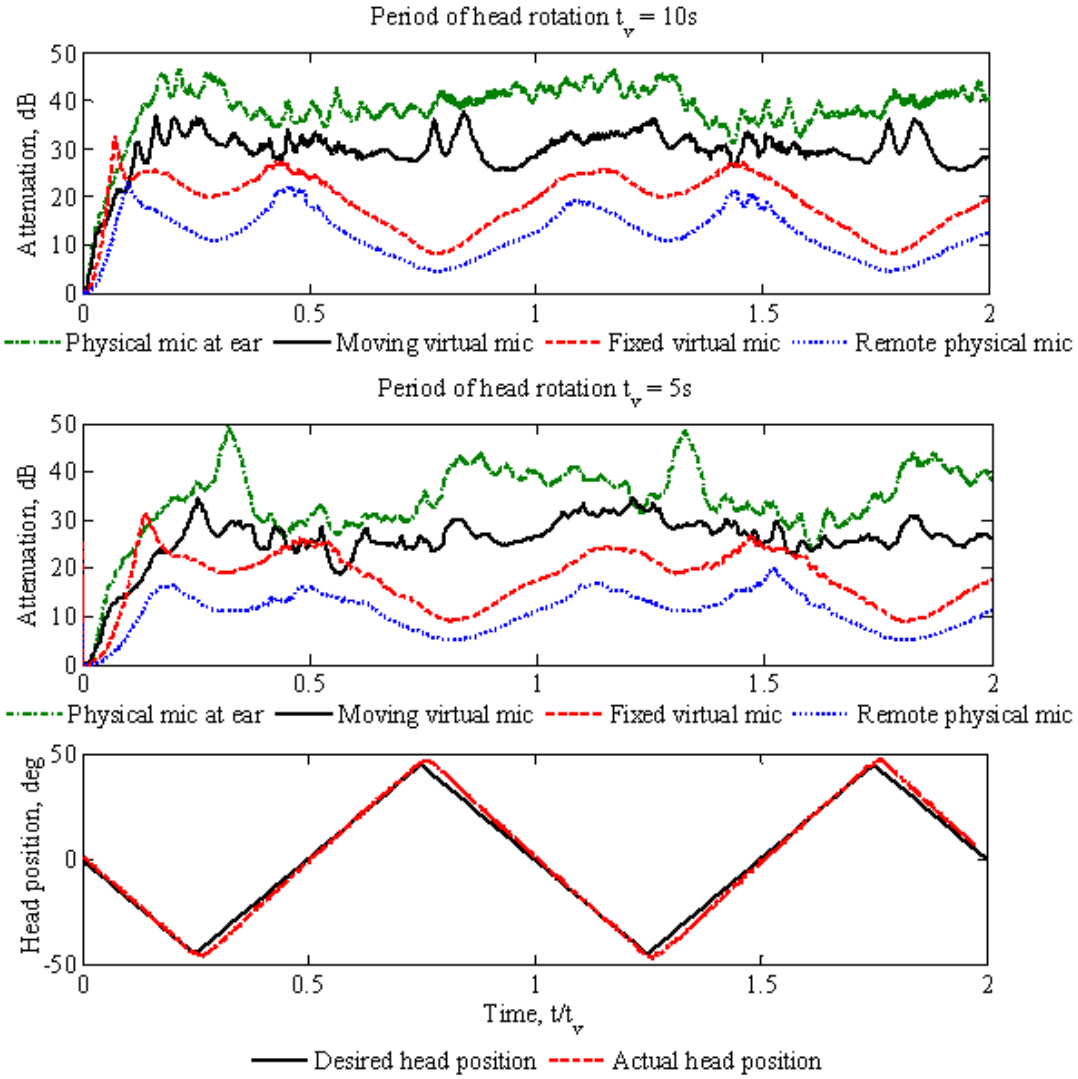

Figure 9: Tonal attenuation achieved at 525 Hz at the moving virtual location for active noise control. t_v = period of head rotation

material and then with metallic or chemically resistant paint. The advantage of using such a protective coating is that it has only a small effect on the output capability of the loudspeaker.

However in abrasive environments, or when steam cleaning is used, protective coatings have a short life and it is necessary to use more robust protection. Such protection may take the form of a membrane mounted between the speaker cone and the environment such that contamination cannot reach the cone as shown in Figure 10. Photos of the speaker enclosure installed in an industrial exhaust stack are shown in Figures 11 and 12.

Careful selection of material is paramount as it needs to be robust so it can withstand any

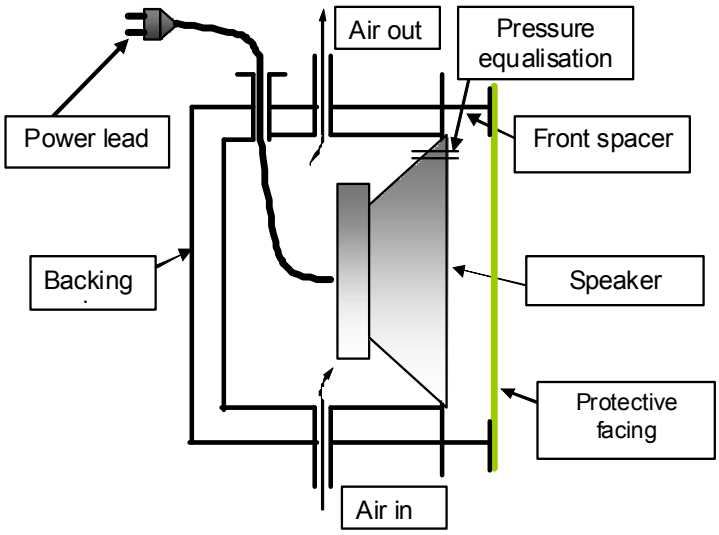

Figure 10: Loudspeaker arrangement for a contaminated environment.

Figure 11: Loudspeaker in its enclosure prior to installation of the mylar protective cover

Figure 12: Speaker mounted in duct wall with a mylar protective cover

cleaning process (including steam cleaning) and it also should not load the speaker and reduce its output capability. Results for the speaker output reduction in dB caused by the application of membranes made using three different materials are given in Table 2 for a particular frequency that was targeted for control in this particular case.

Table 2: Sound reduction at 290 Hz for various protective facings.

Facing material	Thickness (mm)	SPL reduction at 290 Hz
Viton (rubber)	1.5	21.4 dB
Mylar sheet	0.13	2.9 dB
Printed circuit board material	0.1	9.9 dB

To test the durability of speaker unit with Mylar facing in the strong alkali environment, the speaker unit shown in Figures 11 and 12 was mounted on the in-service stack for three and half months. After durability testing the speaker performance was measured on site and it was found that it was the same as when originally installed.

3. EXAMPLES OF INDUSTRIAL ANC SYSTEM IMPLEMENTATION

A. 80 m high Industrial Exhaust Stack radiating a 165 Hz tone

The noise problem was caused by a large, 4m diameter centrifugal fan located at the base of the exhaust stack and which generated a high level tonal noise at the blade pass frequency (BPF). The fan had 10 blades and rotated with a speed of about 993rpm under normal plant operating conditions. The stack was characterised by a normal operating temperature of 100°C which rises to 180°C at times. The exhaust from the fan consists of very moist and abrasive clay dust which sticks to non-vertical surfaces, forming a thick sludge. Attempts at the installation of a passive muffler had not been successful on a long term basis, partly because of the abrasive and sticky nature of the exhaust flow. As the exhaust duct was 3 m wide, higher order modes propagated at the tonal frequency to be controlled. Thus it was decided to install two axial splitters in a section of duct about 2 metres upstream from the fan so that the duct was divided into 3 parallel axial sections, 1 m × 1.2 m in size (see Figure 13). At 100°C, the speed of sound is 388 m/s. For an air flow speed in the duct of 20 m/s, the effective speed of sound is 408 m/s and the wavelength at 165 Hz is 2.47 m so cross modes will not propagate in the divided duct sections.

As the flow in the duct is dirty and sticky, it was necessary to protect the loudspeakers and microphones using similar designs to those discussed in Sections 2F and 2H above. In addition, it was necessary to use an air purge system

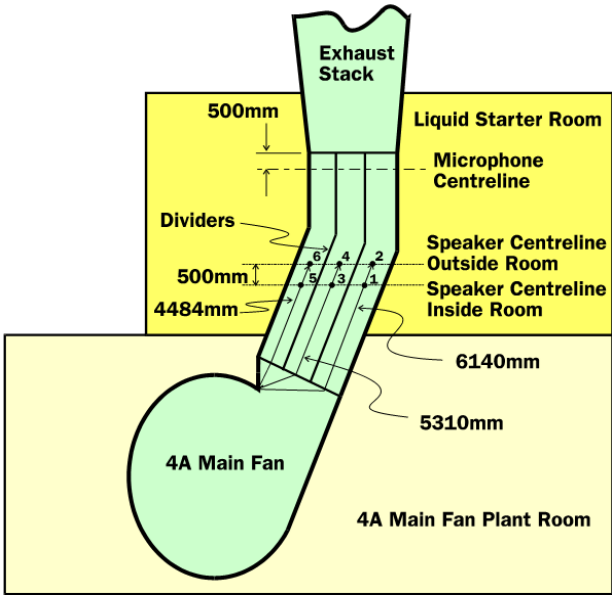

Figure 13: Exhaust stack ANC system layout showing splitters.

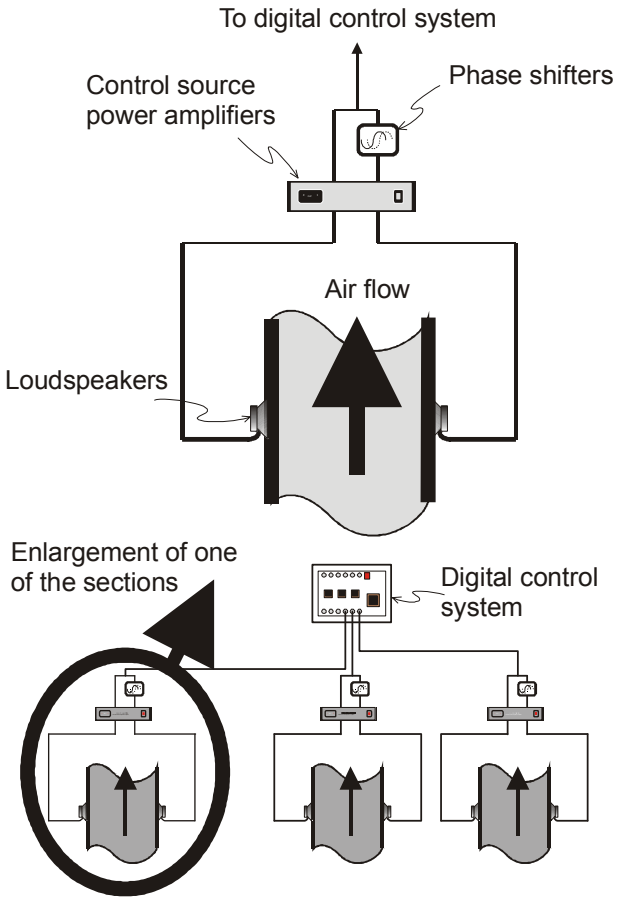

Figure 14: Control system layout for 80 m high exhaust stack ANC.

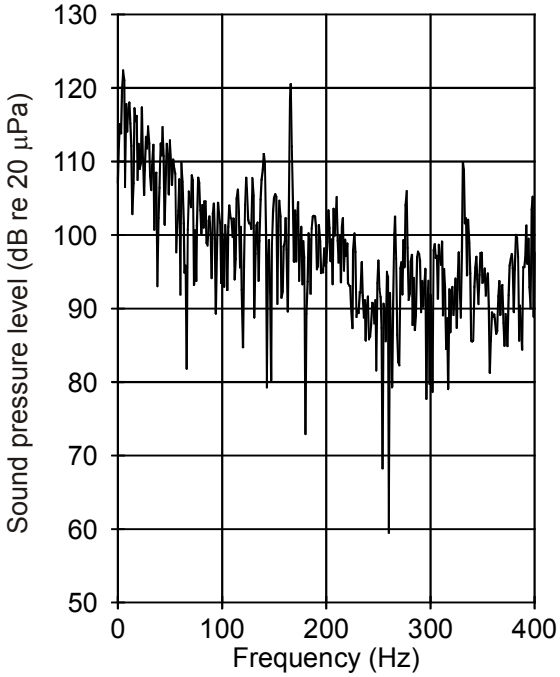

Figure 15: Sound Pressure Level in exhaust stack.

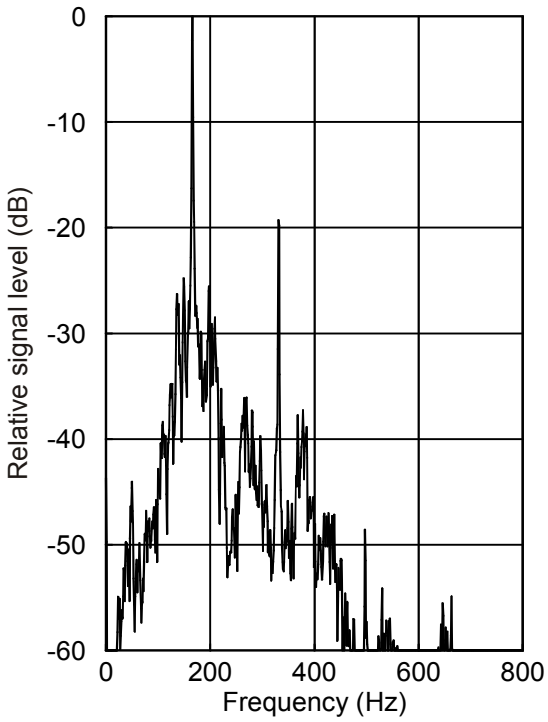

Figure 17: Typical filtered error signal frequency spectrum.

in the microphone housings. More details of these housings are provided elsewhere[21]. As can be seen from Figure 14, two loudspeakers were used for each duct section and each pair was driven by the same control signal. As the loudspeaker characteristics were not identical, it was necessary to insert a phase shifter in the signal line to one of them so the input signal phase could be adjusted so each speaker in a pair was in phase to 0.1 degrees.

It was found necessary to band pass filter the error microphone signal to minimise flow noise effects as illustrated in figures 15 and 16 above. Typical results at one of the error sensors are shown in Figure 17.

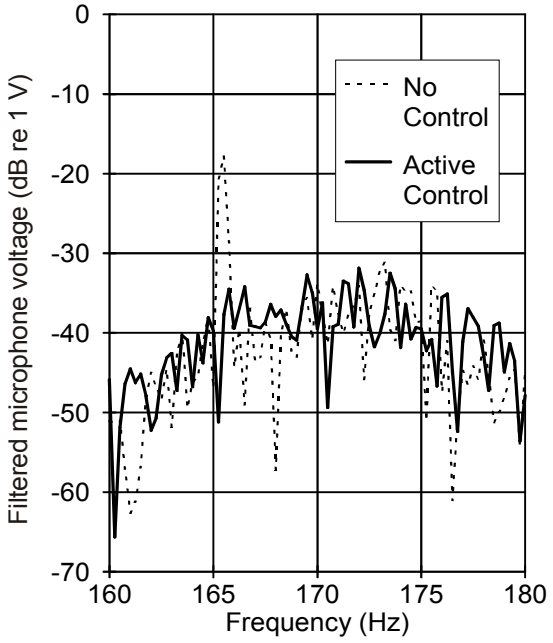

Figure 16: Filtered error microphone voltage in the middle section (duct section 3).

B. Multi-modal ANC in a spray dryer exhaust stack

ANC was implemented to cancel a tone propagating as the first higher order acoustic mode in an exhaust stack of diameter 1.6 m and length 18 m. The first and second cut-on frequencies of the exhaust stack were 127.7 Hz and 212.9 Hz respectively. The stack was driven by a radial type fan with a blade pass frequency varying between 160 to 200 Hz and this was the tone to be controlled via a multi-channel adaptive feedforward controller with 12 error sensor inputs and 6 control outputs, using an FXLMS algorithm with the parameters optimised for this particular problem[23]. The control performance was evaluated in the community surrounding the facility.

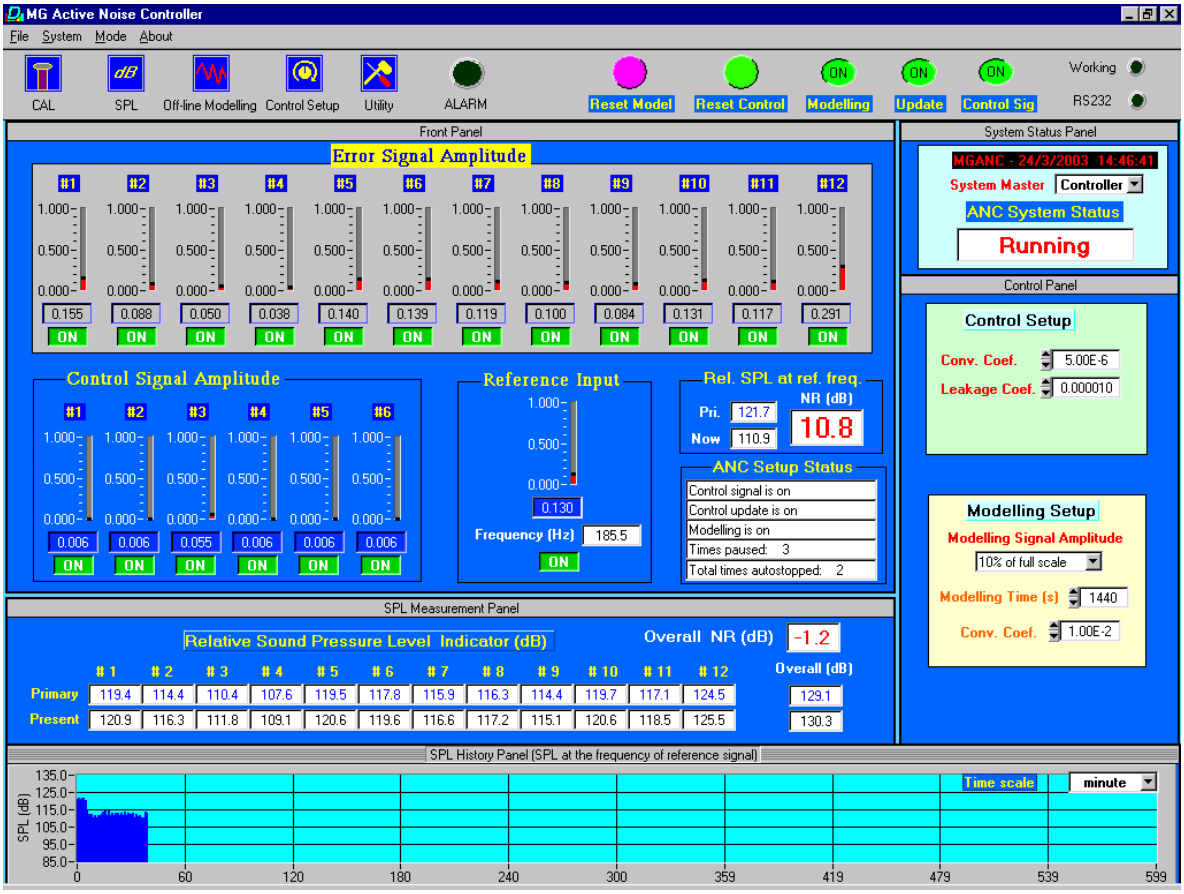

Figure 18: GUI for the control system for the spray dryer exhaust stack.

The error signals were measured using electret microphones mounted on the stack wall. A tachometer signal was used as a reference signal for adaptive feedforward control, where a timing disk mounted on the fan shaft was used to generate an impulse signal, which was used to generate a sine wave signal at the BPF.

Cancellation path modelling was begun using off-line modelling prior to controller start-up. Then after start-up, on-line modelling was begun using very low level (30 dB below the signal level) band limited random noise. This was sufficient to track the changes in the cancellation path that occurred during start-up and operation of the fan.

The graphical user interface (GUI) designed especially for this application is shown in Figure 18. This GUI demonstrates many of the aspects of the system implementation that must be considered if success is to be achieved. Examples include: monitoring of reference sensor output level, error sensor output levels and control source input levels to ensure that output and input amplifier gains are optimally set; ANC system status so that it can be instantly seen if off-line modelling is being undertaken or if the ANC system is operating to cancel the error signals; convergence and leakage coefficient sizes; average of error sensor outputs before and after control for both the tonal frequency to be controlled and overall sound pressure levels to determine the system performance; indication of whether or not each control source and error sensor is operating; and details of the on-line modelling signal amplitude and spectrum. In addition, it is necessary to include a capability for pausing the control system in the presence of excessive transients in the error signals, inspecting the control system panel from a remote location and the ability to start the controller automatically after a power failure.

Other necessary capabilities are reflected by the row of buttons in the second menu line in Figure 18. These include capabilities to: calibrate microphones; do off-line cancellation path

modelling prior to system start-up; set up control system variables such as the convergence coefficient and leakage coefficient; reset the cancellation path model; reset the control system filters; turn the control signal on or off; turn off or turn on the updating of the cancellation path model; turn off or turn on the updating of the control filters; and turning off or on the control signal (to quickly determine the difference between primary and controlled sound pressure levels at the error sensors (as well as in the community).

Practical problems encountered include: cooling air supply contaminated with oil, moisture and particulates; transient pressure surges in cooling air resulting in destroyed speaker cones; and contamination of reference and error signals by extraneous electrical noise from cables carrying heavy current supplies to various items of equipment running on the same cable trays as reference and error signals.

Typical results for one community location are shown in Figure 19 and Table 3 shows the noise level reductions measured at a number of other community locations. It should be noted that the noise level reductions at locations #1-2 and #6-9 are not shown in the table because no significant tones at the BPF were measured at these locations. Substantial control of the tone at the fan blade passing frequency was achievable, even though the tonal frequency was above the first mode cut on frequency of the exhaust stack. The blade passing frequency also varied significantly in amplitude and frequency over short periods of time, so the sound field in the stack could be described as unsteady. The results demonstrated that wherever it could be measured in the community, the fan tone was reduced almost to the background noise level using the active control system.

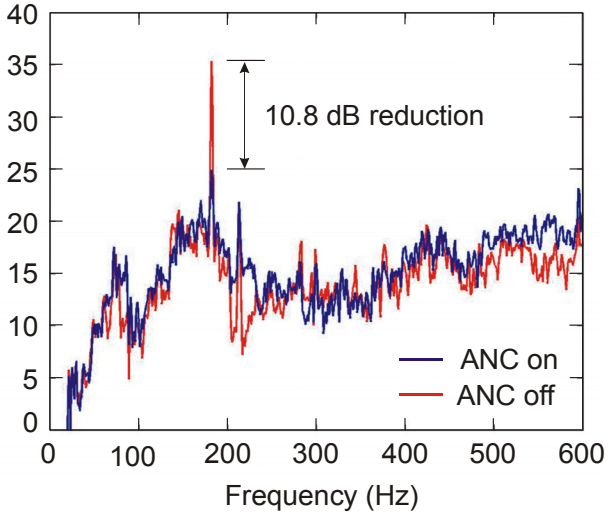

Figure 19: Community noise reduction achieved by the controller on the spray dryer exhaust stack.

Table 3: Noise reduction in the community (dB(A)).

Location	3	4	5	10	11	12	13
Noise level reduction	10.3	12.9	8.6	14.5	13.6	11.6	8.3

4. CONCLUSIONS

Acoustics is a rich field in terms of the potential for improving the quality of life for everyone. In this paper one small aspect has been discussed: the practical implementation of active noise control systems in an industrial environment. There is still a long way to go before this technology will be sufficiently sophisticated and reliable to become an off-the-shelf item in the same way as passive noise control hardware. Further research and development work is needed in all areas associated with ANC implementation, including sound sources, sound sensors, reference signal generation, cancellation path ID algorithms, control algorithms, automatic sound source and sensor configuration optimisation and controller hardware. The reduction in cost and reliability of all of these parts also needs some attention if the technology is to become widely used.

ACKNOWLEDGEMENTS

The author gratefully acknowledges the assistance of his colleagues at The University of Adelaide in carrying out the projects mentioned here. In particular he would like to acknowledge Danielle Moreau for providing Figures 7,8 and 9

REFERENCES

1. C.H. Hansen, Understanding Active Noise Cancellation, Spon Press, London 2001.
2. C.H. Hansen, “Does active noise control have a future?”, in *Proceedings of WESPAC8*, Melbourne, Australia, 2001, paper N° AP2.
3. S.M. Kuo and D.R. Morgan, Active Noise Control Systems, John Wiley, New York 1996.
4. L.J. Eriksson, Development of the filtered-u algorithm for active noise control, *Journal of the Acoustical Society of America* **89**, pp. 257-265, (1991).
5. L.J. Eriksson, M.C. Allie and R.A. Greiner, The selection and application of an IIR filter for use in active sound attenuation, *IEEE Transactions on Acoustics, Speech and Signal Processing* **ASSP-35**, pp433-437, (1987).
6. D.R. Morgan and J.C. Thi, "A delayless sub-band adaptive filter architecture", in *IEEE Trans. Signal Processing*, **43**, pp. 1818-1830 (1995).
7. S.J. Park, J.H. Yun and Y.C. Park, "A delayless sub-band active noise control system for wideband noise control", *IEEE Trans. Speech and Audio Processing*, **9**, pp. 892-899 (2001).
8. X. Qiu, L. Ningrong, G. Chen and C.H. Hansen, "The implementation of delayless subband active noise control algorithms", in *Proceedings of Active '06*, Adelaide, Australia, 2006.
9. X. Qiu and C.H. Hansen, “Multidelay adaptive filters for active noise control”, in Proceedings of the *14th International Congress on Sound and Vibration*, Cairns, Australia, 2007, paper N° 140.
10. S. J. Elliott, Signal Processing for Active Control, Academic Press, London, 2001.
11. C.H. Hansen, “Active noise control - from laboratory to industrial implementation”, in *Proceedings of Noise-Con '97*, Penn State Univ, pp. 3-38, 1997.
12. C.H. Hansen, X. Qiu, G. Barrault, C.Q. Howard, C. Petersen and S. Singh, “Optimisation of active and semi-active noise and vibration control systems”, in *Proceedings of the 14th International Congress on Sound and Vibration*, Cairns, Australia, 2007.
13. C.H. Hansen, C.Q. Howard, K.A. Burgemeister and B.S. Cazzolato, “Practical implementation of an active noise control system in a hot exhaust stack”, in *Proceedings of the Annual Meeting of the Australian Acoustical Society*, Brisbane, (1996).
14. S.J. Elliott, A. David, “A virtual microphone arrangement for local active sound control”, in *Proceedings of the First International Conference on Motion and Vibration*, 1027-103, 1995.
15. A. Roure, A. Albarrazin, “The remote microphone technique for active noise control”, in *Proceedings of Active 99*, 1233-1244, 1999.
16. B.S. Cazzolato, “An adaptive LMS virtual microphone”, in *Proc. of Active 02*, 105-116, 2002.
17. C.D. Petersen, R. Fraanje, B.S. Cazzolato, A.C. Zander, C.H. Hansen, “A Kalman filter approach to virtual sensing for active noise control”, *Mechanical Systems and Signal Processing*, **22**, 490-508, (2007).
18. C.D. Petersen, B.S. Cazzolato, A.C. Zander, C.H. Hansen, “Active noise control at a moving location using virtual sensing”, in *Proc. 13th Int. Congress of Sound and Vibration*, Vienna, 2006.
19. C.D. Petersen, A.C. Zander, B.S. Cazzolato, C.H. Hansen, “A moving zone of quiet for narrowband noise in a one-dimensional duct using virtual sensing”, *Journal of the Acoustical Society of America*, *121*, 1459-1470, (2007).
20. D. Moreau, A.C. Zander and B.S. Cazzolato, “Active noise control at a moving virtual sensor in three-dimensions”, *Acoustics Australia*, **36**, 93-96, (2008).
21. C.H. Hansen, C.Q. Howard, K.A. Burgemeister and B.S. Cazzolato, “Practical implementation of an active noise control system in a hot exhaust stack”, in *Proceedings of the Annual Meeting of the Australian Acoustical Society*, Brisbane, 1996.
22. X. Qiu, X. Li, D.L.L. Leclercq, A.C. Zander, C.D. Kestell and C.H. Hansen, “Robust design of active noise control system on a spray dryer exhaust”, in *Proceedings of Active 2002*, Southampton, 2002, pp.749–760.
23. X. Li, X. Qiu, X., D.L.L. Leclercq, A.C. Zander and C.H. Hansen, “Implementation of active noise control in a multi-modal spray dryer exhaust stack”, *Applied Acoustics*, **67**, 28-48, (2006).